Materials Research Express

PAPER

Parameter optimization and characterization of environmental friendly aluminium hybrid metal matrix composites

RECEIVED
28 June 2019

REVISED
4 October 2019

ACCEPTED FOR PUBLICATION
21 October 2019

PUBLISHED
1 November 2019

Girija Moona[1,3], **R S Walia**[1,2], **Vikas Rastogi**[1] **and Rina Sharma**[3]

[1] Delhi Technological University, New Delhi-110042, India
[2] Punjab Engineering College, Chandigarh, India
[3] CSIR- National Physical Laboratory, Dr K. S. Krishnan Marg, New Delhi-110012, India

E-mail: moonag@nplindia.org

Keywords: Hybrid composites, Reinforcement, Electromagnetic stirring, Metal matrix composites, Optimization

Abstract

The present experimental investigation was carried out to fabricate environmental friendly hybrid aluminium metal matrix composites with three reinforcements in minimal amount through electromagnetic stir casting: an uncommon fabrication technique. Al 7075-T6 alloy was infused with three reinforcements; eggshell particles (wt% 0.5, 1 and 1.5, particle size ~60 μm), SiC particles (wt% 1, 1.5 and 2, particle size ~65 μm) and Al_2O_3 particles (wt% 1.5, 2 and 2.5, particle size ~90 μm) with variable mechanical stirring time (2, 4 and 6 min). Composite fabrication experiments were run in accordance with Taguchi's orthogonal array L9 and analysis of variance (ANOVA) was conducted to optimize process parameters and to observe their influence on quality characteristics. Developed composites were characterized for various physical and mechanical properties such as density, porosity, residual stress, micro hardness and tensile strength. Investigation outcomes show that synthesized hybrid composite specimen S8 with a total reinforcement content of 4.5% only, demonstrated no significant change in density (only upto 2.2%) whereas the maximum reduction in percentage porosity was 75%. Additionally, maximum abatement in residual stress of hybrid composite specimen S8 was 76% as compared to their unreinforced counterpart specimen S0, there was a maximum enhancement of 83% in microhardness and 107% in tensile strength of fabricated hybrid aluminium metal matrix composite specimen S8 in comparison of as-cast Al 7075-T6 specimen S0. Disposal of eggshells is a serious threat to environment, thus more focus was put on recycling them and using them for development of environmental friendly and cost effective hybrid composites with enhanced properties for numerous engineering applications.

1. Introduction

In present scenario, metal matrix composites are replacing their conventional counter parts in a flashing way in most of the advanced engineering applications due to their augmented mechanical properties [1]. Aluminium alloys as base metals can be infused using fibers, whiskers and particulate reinforcements [2]. A wide range of particulate reinforcements such as TiB_2, B_4C, SiC, Al_2O_3, TiC, TiO_2, WC, graphite, fly ash, red mud, rice husk ash, bamboo leaf ash and bagasse ash etc have been used to develop aluminium metal matrix composites with enhanced properties [3]. Al 7075 mixed with B_4C particles through stir casting route showed increased hardness and wear resistance, whereas Al 7075 infused with TiB_2 particles displayed increased micro hardness, tensile strength and yield strength [4]. In another study Al 7075 alloy with SiC particles was analyzed for wear behavior and surface finish and it was observed that for higher content of reinforcement the tool wear was increased and surface finish became inferior [5]. Established AMMCs with single reinforcement exhibit enhanced characteristics but often compromise with other crucial properties, hence hybrid composites have been developed keeping in view the reasonable enhancement in properties by exploiting different virtues of various reinforcements without any noticeable deterioration in composite attributes [6]. Addition of SiC particles into aluminium alloys increases mechanical strength and wear resistance but at the cost of ease of machining. Whereas Al-SiC-Gr hybrid composites possess improved wear resistance and machinability both [7]. Hybrid composites of aluminium alloy with SiC and B_4C particles fabricated through ultrasonic cavitation based solidification process exhibited enhanced hardness and higher tensile strength. Aluminium composite with SiC and bamboo leaf ash, developed by two step stir casting method showed decreased density and improved corrosion resistance [8]. Al 2219/B_4C/MoS_2 hybrid composites showed decreased densities, increased microhardness and better wear resistance. With enhanced thermal stability, Al/Zn/Al_2O_3 stir casted hybrid composites have wide utilizations in precision applications and thermal packaging [9].

Among various fabrication techniques for development of particulate reinforced aluminium metal matrix composites, stir casting is considered to be the most advantageous due to its cost effectiveness, ability to handle large volume, simplicity and capacity to control metal matrix structure. In stir casting process composites are produced by continuous stirring of base metal melt followed by infusion of reinforcements [10, 11]. The desired particulate reinforcements with reasonable wettability are incorporated into molten aluminium matrix and the mixture is solidified. Composites developed by stir casting technique demonstrate modifiable properties depending upon distinct process parameters such as reinforcement content, reinforcement preheat temperature, stirring temperature, stirring time, stirring speed and stirrer position etc [12]. Fundamental complications experienced during stir casting are improper wetting due to poor interfacial bonding between reinforcement & metal matrix and non-uniform distribution of reinforcement particles due to agglomeration [13]. To improve interfacial bonding of filler and metal matrix, various surface treatments were performed including ultrasonic cavitation effect and inclusion of nanostructures into composites while for enhanced wettability, either alloying elements were added to molten metal matrix or coating of reinforcements was carried out [14, 15]. Even with such critical corrective actions, sometimes in stir casting process the reinforcement particles get repelled away from the mechanical stirrer due to the centrifugal force of rotating melt resulting into non uniform dispersion [16]. To overcome this complication, in current study, modifications were implemented to existing mechanical stir casting setup in form of electromagnetic stirrer. In electromagnetic stirrer, a three phase motor with the help of alternating current generated rotational motion and applied rotational force on reinforcement particles infused in molten metal resulting into uniform dispersion of particulate reinforcements in metal matrix. In order to enhance mechanical attributes of developed hybrid composites and avert agglomeration, hard particles of comparable sizes (eggshell particles with particle size $\sim$60 μm, SiC particles with average particle size $\sim$65 μm and Al_2O_3 particles with average particle size $\sim$90 μm) were used as reinforcements. Hybrid aluminum metal matrix composites prepared using electromagnetic stirring were evaluated for porosity, as porosity is a defect caused by interfacial reactions of preform and metal matrix inducing decline in mechanical characteristics of composites. Hence investigations for density and percentage porosity of fabricated hybrid aluminium composites were important measures [17]. Also the analysis of residual stress of hybrid composites was extremely momentous as they cause dimensional distortions and diminished mechanical characteristics [18]. Sequentially, fabricated hybrid aluminium composites were evaluated for microhardness, tensile strength and fractographic studies. Developed hybrid composites with light weight and enhanced strength may replace conventional alloys in aerospace and automobile industry for manufacturing of specific parts such as wing slat tracks, bulkheads, landing gears, wheels, piston cylinder liners, transmission housings, connecting rods, suspension components and brakes etc and also for fabrication of numerous structural components likewise platforms, bridges, power plant structures, offshore structures and roof structures.

In present industrial scenario, a humongous research gap can be observed for development of eco-friendly materials with distinctive mechanical attributes to cater specialized needs. In reference to hybrid aluminium metal matrix composites, literature on few conventional fabrication methods, with limited reinforcement combinations (utmost two reinforcements) and higher filler contents is available. Also detailed influence of various reinforcements on a wider range of mechanical traits of developed composites such as percentage porosity and residual stress has not been reported so far. In this backdrop, there is an enormous scope for current research work for development of ecodesigned hybrid aluminium metal matrix composites with upgraded mechanical properties using three reinforcements through electromagnetic stir casting route.

2. Experimental procedure

2.1. Setup design

The present experiment for fabrication of aluminium hybrid metal matrix composites was conducted using a combined setup of conventional stir casting system and electromagnetic stirrer. The conventional stir casting setup included a furnace, stirrer impeller (rotating at 150 rpm), temperature sensors and control panel etc. An electromagnetic stirrer originally was an electric motor using a rotating magnetic field causing whirling motion

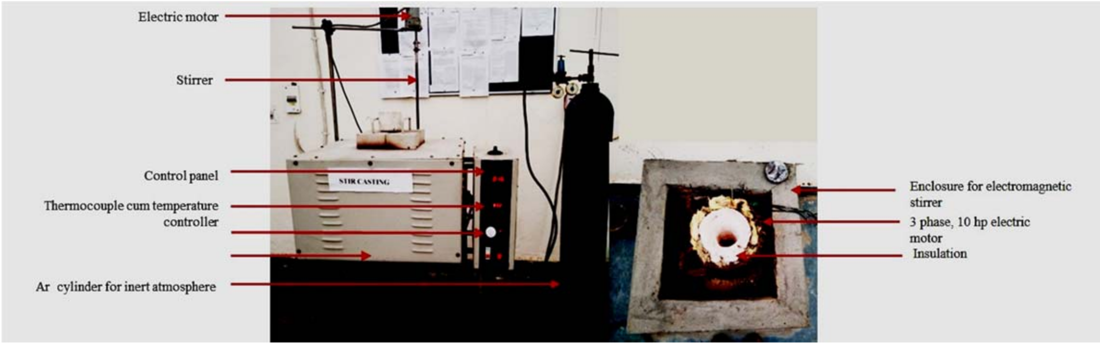

Figure 1. Electromagnetic Stir casting setup.

Table 1. Composition of Al 7075-T6 [19].

Component	Al	Cr	Cu	Fe	Mg	Mn	Si	Ti	Zn	Others
Wt%	87–91	0.18–0.28	1.2–2	>0.5	2.1–2.9	>0.3	>0.4	>0.2	6	Balance

Table 2. Reinforcement details.

Reinforcement	Average particle size (μm)
Egg shell powder	60
SiC powder	65
Al_2O_3 powder	90

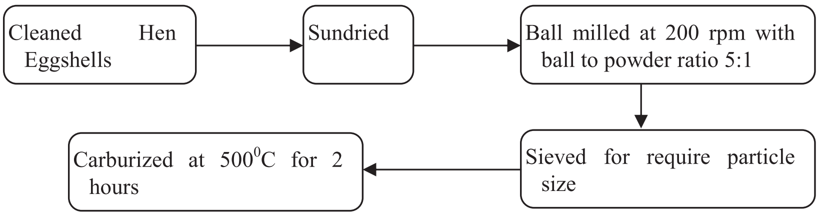

in molten metal. When a three phase AC voltage was applied to the motor, its magnetic coil generated a moving magnetic field and electromagnetic force was developed in the metal melt causing its stirring. In current investigation a three phase 10 hp motor rotating at 960 rpm used as electromagnetic stirrer was combined with mechanical stir casting setup (figure 1).

2.2. Details of selected base metal matrix and reinforcements

2.2.1. Base metal matrix

Previous series of aluminium alloys have already been explored extensively for numerous experimental investigations. The metal matrix used for current study was Al 7075-T6 alloy due to superior physical properties. Synthesized Al 7075-T6 hybrid composites with their ameliorated traits may have extensive spectrum of state-of-the-art applications including high strength structural applications, thermally modifiable & light weight aerospace applications, automotive applications due to better tribological & fatigue properties, electronics applications due to higher specific strength for power electronics & packaging materials and numerous defence applications due to low density, high thermal conductivity, high heat capacity & dimensional stability at higher temperatures. Chemical compositions of Al 7075-T6 alloy is given in table 1 [19].

2.2.2. Reinforcements

Each reinforcement used for current investigation had specific characteristics, thus when mixed with molten metal, they contributed towards enhancement of distinct properties of synthesized composites as compared to the unreinforced metal. Disposal of certain natural waste matter such as eggshells is extremely harmful for our environment, hence after recycling; these can be used as natural reinforcements to develop composites. In

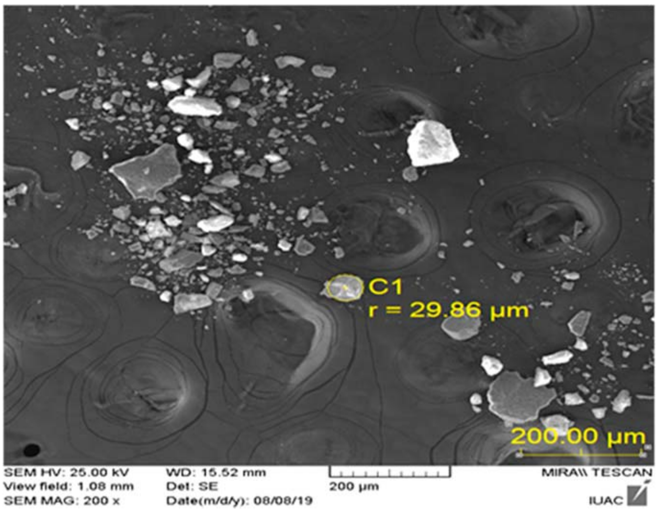

Figure 2. SEM micrograph of eggshell particles.

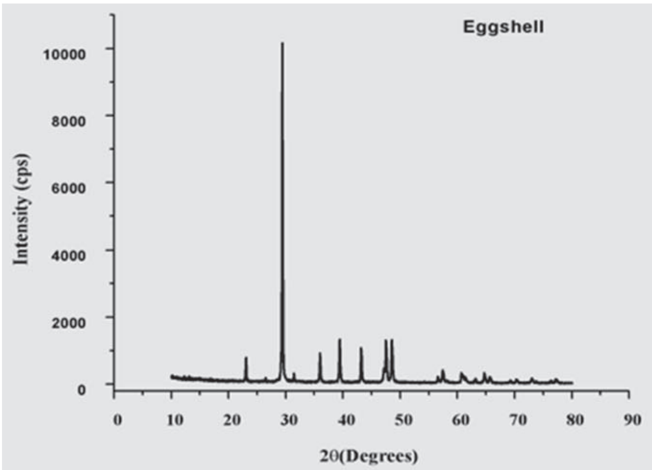

Figure 3. XRD pattern of eggshell particles.

present experiment, hybrid aluminium metal matrix composites were prepared by infusing three fillers in order to tailor the properties of fabricated composites as per desired applications. Details of reinforcements used in the experiment are given in table 2.

Microstructural and elemental analysis of reinforcement particles using field emission scanning electron microscope (Make: OXFORD Instruments, Model: 7718) and x ray diffractometer (Make: Rigaku Japan, Model-Miniflex-II) are illustrated in figures 2 to 7. Reinforcement particle sizes were determined by SEM micrographs obtained at 200X magnification. Avergae size of eggshell particles was observed to be ≈60 μm, of SiC particles ≈65 μm and of Al_2O_3 particles ≈90 μm as show in figures 2, 4 and 6. XRD intensity data for all the reinforcements were taken for 2θ range of 10°–100°. For eggshell particles the diffraction peaks are located at 23.58°, 30°, 37.76°, 40°, 44.89° and 50° as shown in figure 3, whereas for silicon carbide particles the intensity peaks occur at 38.52°, 41.96°, 60° and 73.84° as shown in figure 5. In figure 7, the spectrogram of aluminium oxide particles displays distinctive peaks at 25.9°, 35.41°, 37°, 44.25°, 52.72°, 57°, 68.78° and 77°.

2.3. Composite preparation

Here, 9 hybrid aluminium composites were fabricated using Al 7075-T6 as metal matrix infused with variable weight percentage of three reinforcements (eggshell particles weight percentage 0.5%, 1%, 1.5%, average particle size ~60 μm, SiC particles weight percentage 1%, 1.5% and 2%, average particle size ~65 μm and Al_2O_3 particles weight percentage 1.5%, 2% and 2.5%, average particle size ~90 μm) with varied mechanical stirring time

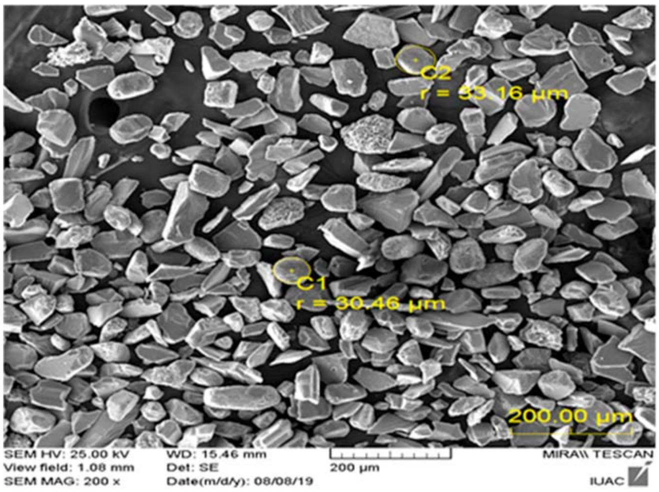

Figure 4. SEM micrograph of SiC particles.

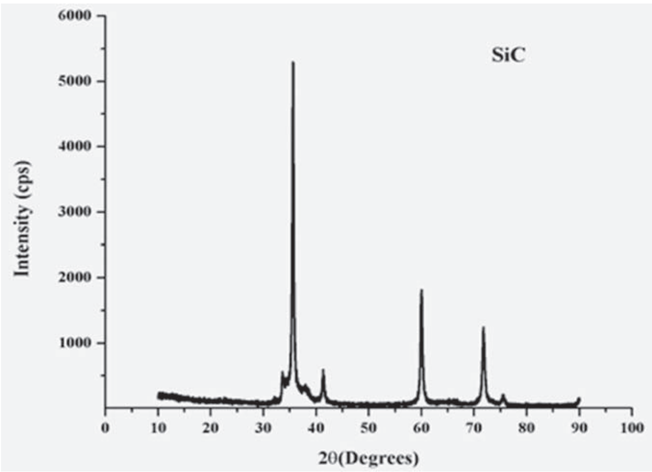

Figure 5. XRD pattern of SiC particles.

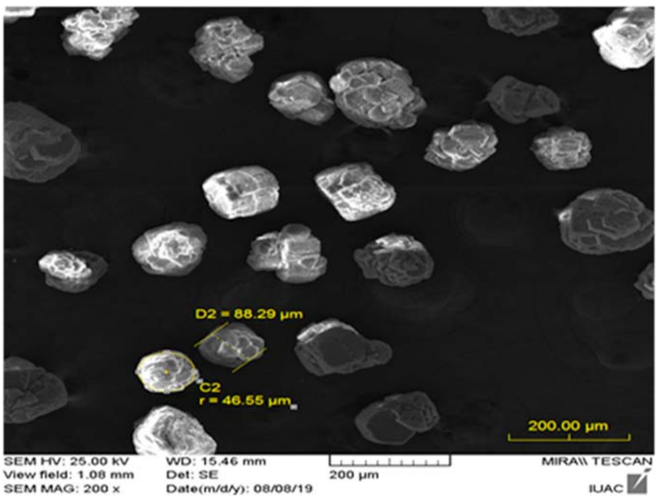

Figure 6. SEM micrograph of Al_2O_3 particles.

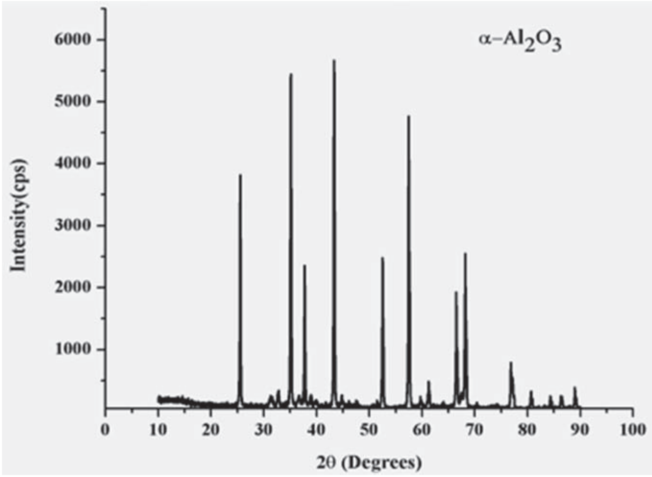

Figure 7. XRD pattern of Al_2O_3 particles.

Table 3. Design of experiment layout.

Hybrid composite specimen number	Eggshell wt%	SiC wt%	Al_2O_3 wt%	Mechanical stirring time (minutes)
S1	0.5	1	1.5	2
S2	0.5	1.5	2	4
S3	0.5	2	2.5	6
S4	1	1	2	6
S5	1	1.5	2.5	2
S6	1	2	1.5	4
S7	1.5	1	2.5	4
S8	1.5	1.5	1.5	6
S9	1.5	2	2	2
S0			As-cast Al 7075-T6	
Mechanical stirring speed			150 rpm	
Stirring temperature			850 °C	
Reinforcement preheat temperature			500 °C	
Electromagnetic stirring speed			960 rpm	
Electromagnetic stirring time (minutes)			0.5	

(2 min, 4 min and 6 min) in accordance with the design matrix using Taguchi L9 orthogonal array as shown in table 3. An L9 orthogonal array was appropriate for this experiment as it was conducted to figure out the effect of four independent factors (eggshell particles wt%, SiC particles wt%, Al_2O_3 particles wt% and mechanical stirring time) with three different factor level values assuming that there is no cross product effect between any two factors [20].

To fabricate composites, aluminium ingots were cleaned and melted in crucible in an electric furnace at 900 °C. Meanwhile required amount of reinforcements were wrapped in aluminium foil and preheated in a muffle furnace up to 500 °C for 1 h in order to remove absorbed gases from reinforcements surface, avoid temperature drop on infusion of reinforcement particles into molten metal and obtain improved wettability. The temperature of metal melt was slightly reduced and reinforcements were added in 3 steps. A preheated stirrer was used to stir the mixture in inert atmosphere at 150 rpm for variable time intervals as per the design of experiment. After mechanical stirring, the crucible was placed on electromagnetic stirrer rotating at 960 rpm for 30 s for electromagnetic stirring in inert atmosphere. The composite castings (figure 8) were allowed to solidify and various test specimens were prepared as per standard sizes for mechanical testing.

In order to evaluate mechanical and physical characteristics of composites, ten specimens (one as-cast Al 7075-T6 and nine Al 7075-T6/egg shell/SiC/Al_2O_3 hybrid composites, in three replications) for each characterization were prepared. For density, porosity, residual stress and micro hardness testing, specimen palates (conventionally polished up to Ra $\sim$ 0.1 μm) of size $10 \times 10 \times 5$ mm^3 were prepared (figure 9), whereas for tensile testing the sub-size dog bone plate type specimens were prepared as per ASTM E8-M11 (figure 10).

Figure 8. Composite castings.

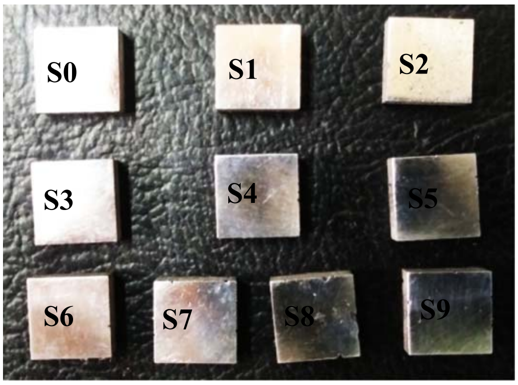

Figure 9. Specimens for density, porosity, micro hardness and residual stress testing.

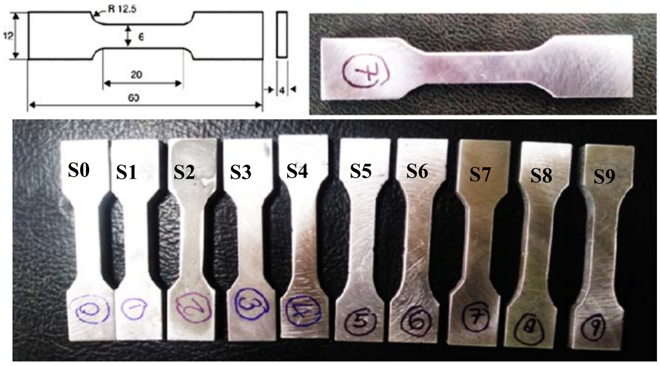

Figure 10. Specimens for tensile testing (all the dimensions are in mm).

3. Results and discussions

Taguchi method is based on predefined instructions and uses a set of arrays to designate a procedure for carrying out minimum number of experiments being able to provide complete information related to the performance parameters. In Taguchi approach, for an orthogonal experimental design the influence of control factors can be segregated in terms of S/N ratio and mean response [20, 21]. Mean objectives/response functions were analysed using data from designed experiments in order to calculate signal to noise (S/N) ratio. Analysis of variance (ANOVA) was conducted to investigate the influence of process parameters on specific quality characteristics in

Table 4. Factors and their levels.

Control factors	Factors designation	Level 1	Level 2	Level 3
Eggshell weight %	A	0.5	1	1.5
SiC weight %	B	1	1.5	2
Al_2O_3 weight %	C	1.5	2	2.5
Mechanical stirring time (minutes)	D	2	4	6

terms of F-ratio and percentage contribution. All the four control factors with three levels (because they may affect the performance attributes nonlinearly) are shown table 4.

3.1. Prediction of optimum Porosity in fabricated hybrid composites

Density measurement was done using gravimetric method/hydrostatic weighing method as per standard OIML-r111 on a Mettler Toledo weighing balance. At recorded temperature, each specimen was first weighed in air and then weighed in distilled water. Density of distilled water is calculated by an empirical formula given in equation (1).

$$\rho_1 = 0.99997495\left[1 - \frac{(t - 3.983035)^2(t + 301.797)}{522528.9X(t + 69.348.81)}\right] \quad (1)$$

Where t: Recorded temperature

Density of each test specimen was obtained by equation (2).

$$\rho_t = \frac{(I_{ta} \times \rho_l) - (I_{tl} \times \rho_a)}{I_{ta} - I_{tl}} \quad (2)$$

Where ρ_t: Density of test specimen at recorded temperature

ρ_l: Density of distilled water at recorded temperature

ρ_a: Density of air at recorded temperature

I_{ta}: Weight of specimen in air at recorded temperature

I_{tl}: Weight of specimen in distilled water at recorded temperature

Theoretical values of density for hybrid composites were calculated by using rule of mixtures [22], explained by equation (3).

$$\frac{1}{\rho_c} = \frac{1}{\rho_{f1}}\left(\frac{w_{f1}}{w_c}\right) + \frac{1}{\rho_{f2}}\left(\frac{w_{f2}}{w_c}\right) + \frac{1}{\rho_{f3}}\left(\frac{w_f3}{w_c}\right) + \frac{1}{\rho_m}\left(\frac{w_m}{w_c}\right) \quad (3)$$

Where ρ_c and w_c: Density and weight of composite

ρ_{f1} and w_{f1} : Density and weight of eggshell powder

ρ_{f2} and w_{f2}: Density and weight of Silicon carbide

ρ_{f3} and w_{f3}: Density and weight of Aluminium Oxide

ρ_m and w_m: Density and weight of Al 7057-T6 alloy used as metal matrix

Percentage porosity of developed composites was calculated by expression given in equation (4) [22].

$$\%\ \text{Porosity} = \left\{\left(\frac{\rho_T - \rho_{EX}}{\rho_t}\right)\right\} \times 100\% \quad (4)$$

Here ρ_T: Theoretical density of composite

ρ_{EX}: Experimental density of composite

Experimentally obtained and theoretically calculated mean values of density for as-cast Al 7075-T6 specimen and 9 composites specimens (in three replications) are shown in figure 11. It was observed that there was no significant change in density of composites as compared to the base metal (only upto 2.2%) due to comparable densities of infused reinforcements.

Table 5 shows three readings corresponding to three raplications for percentage porosity measurement of developed hybrid composite specimens with respective S/N ratio for 'smaller the better' type of quality characteristic. Plots in figure 12 demonstrate the effect of different process parameters on S/N ratio and percentage porosity. It is displayed that for increased reinforcements content (figures 12(a)–(c)) and longer mechanical stirring time (figure 12(d)) percentage porosity of developed hybrid aluminium metal matrix

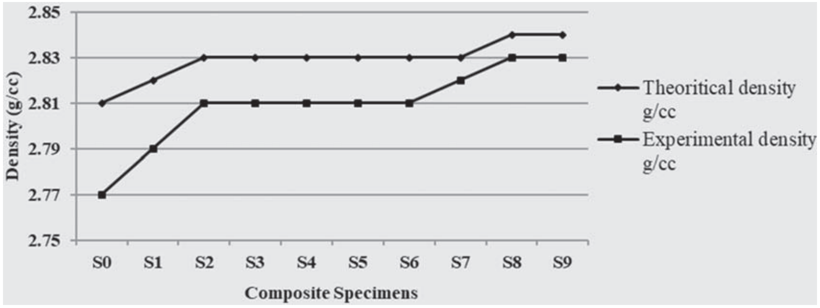

Figure 11. Density of composites.

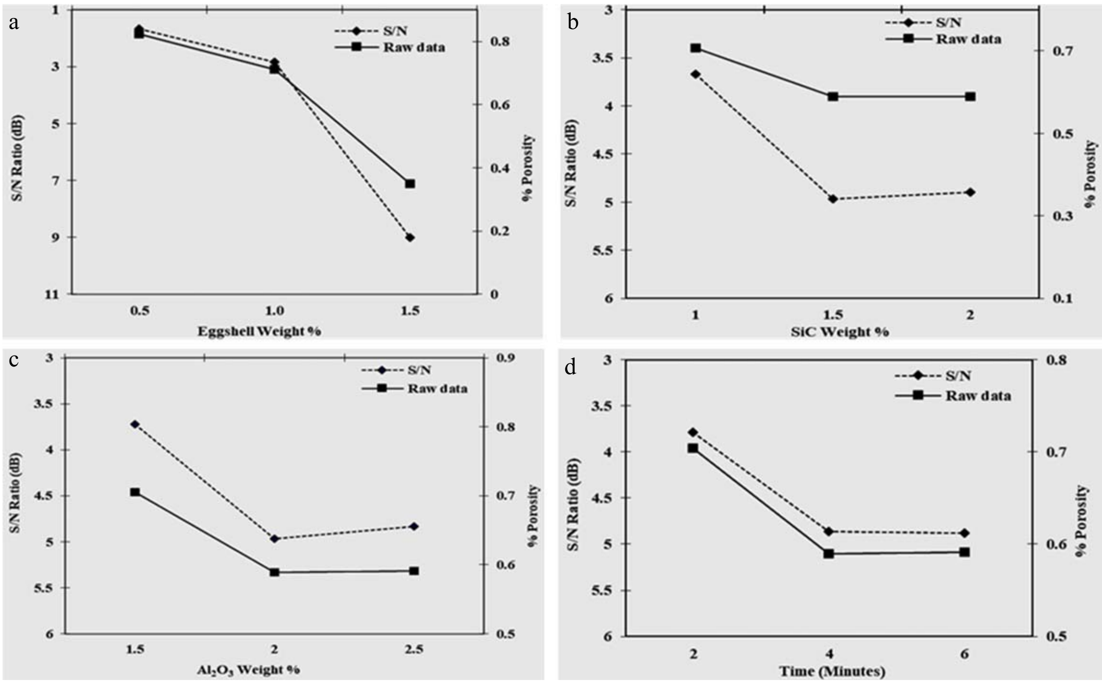

Figure 12. Effect of (a) Eggshell wt% (b) SiC wt% (c) Al_2O_3 wt% (d) mechanical stirring time on percentage porosity and S/N ratio.

Table 5. Observations for percentage porosity and S/N ratio.

Percentage porosity					
Average percentage porosity of as-cast Al7075-T6 Specimen S0: 1.42					
Composite specimen	Reading 1	Reading 2	Reading 3	Mean	S/N ratio (dB)
S1	1.35	1.03	0.79	1.06	−0.67
S2	0.83	0.67	0.62	0.71	2.94
S3	0.7	0.91	0.52	0.71	2.76
S4	0.86	0.6	0.68	0.71	2.83
S5	0.61	0.84	0.68	0.71	2.89
S6	0.88	0.73	0.52	0.71	2.79
S7	0.45	0.27	0.34	0.35	8.84
S8	0.29	0.37	0.39	0.35	9.05
S9	0.35	0.4	0.29	0.35	9.12

composites was decreased. It was inferred that for minimum percentage porosity and S/N ratio, 3^{rd} level of eggshell content (A_3), 2^{nd} level of SiC content (B_2), 2^{nd} level of Al_2O_3 content (C_2) and 2^{nd} level of mechanical stirring time (D_2) were optimum levels. ANOVA is a statistical technique that is capable of analysing any

Table 6. Analysis of variance (ANOVA) for percentage porosity.

Factor	Sum of squares (SS)	Degrees of freedom	Variance (V)	Percentage contribution (P)	F-Ratio
Eggshell Wt%	1.11	2	0.55	54.32	46.27
SiC Wt%	0.17	2	0.08	8.26	7.04
Al_2O_3 Wt%	0.17	2	0.09	8.62	7.34
Stirring time	0.37	2	0.19	18.23	15.53
Others/errors	0.21	18	0.01	10.57	—
Total	2.03	26	—	100	—

Table 7. Confirmation experiment for percentage porosity.

Quality characteristic	Replications			
Percentage porosity of composites	Replication 1	Replication 2	Replication 3	Mean
	0.57	0.29	0.32	0.39

experimental data and drawing significant conclusions in terms of F ratio, percentage contribution and error variance [23, 24]. Table 6 shows ANOVA results computed at 95% confidence level, it demonstrates F-ratio and percentage contribution of various factors toward quality characteristic. It was noticed that eggshell wt% (P = 54.32%) had significant effect and mechanical stirring time (P = 18.23%) had moderate influence on porosity of synthesized hybrid composites where as other control factors were insignificant.

In can be observed from graphs in figure 12 that the insignificant control factors had almost horizontal lines while the significant control factors had lines with higher inclinations [25, 26]. After analysing S/N ratio and mean response characteristic, optimum levels of physically and statistically significant factors were determined to be A_3 and D_2. The predicted mean of percentage porosity at optimal level of process parameters was enumerated using equation (5) [27, 28].

$$X_{mp} = \overline{G} + (\overline{A_3} - \overline{G}) + (\overline{D_2} - \overline{G}) \tag{5}$$

Here X_{mp} denoted the predicted mean of percentage porosity at optimum condition and $\overline{G}$ was the grand average of all 27 observations of utility characteristics from table 5. $\overline{A_3}$ and $\overline{D_2}$ represented the average values of percentage porosity at optimal level of significant process parameters. On submitting estimated values of various response averages as $\overline{G} = 0.63$, $\overline{A_3} = 0.35$ and $\overline{D_2} = 0.59$ in equation (5), predicted mean optimum value of percentage porosity was realized to be 0.311. From table 6 the values were obtained for error variance (0.01) and degree of freedom (DOF) for error (18) whereas F-ratio value at 95% confidence interval was determined from standard statistical table. Further, confidence interval (CI) was calculated to be ±0.19. Hence confidence interval with respect to 95% confidence level of predicted optimum percentage porosity was 0.121 < percentage porosity (PP) < 0.5. In accordance with Taguchi's optimization approach, a confirmation experiment was conducted by running three more replications for percentage porosity of developed hybrid composites at optimal levels of process parameters as given in table 7 in order to authenticate the predicted results. It is realized from table 7 that confirmation experiment result obtained for percentage porosity of composites was covered within the predicted confidence interval $0.121 < PP < 0.5$.

3.2. Prediction of optimum Residual Stress in fabricated hybrid composites

Residual stress might occur in fabricated hybrid composite specimens due to temperature gradients and machining forces resulting into premature failure. Measurements of residual stresses in specimens were carried out by x-ray diffraction technique using a non-destructive x-ray analyser (μ-X360) as shown in figure 13(a). It consists of a position sensitive detector unit with scintillation counter for measuring the residual stress in metallic surfaces by detecting and comparing the full Debye ring data (figures 13(b)–(e)) from a single incident x-ray angle with non-stressed state. X ray diffraction method determined the residual stress by measuring the distance between crystallographic planes using the angles at which maximum intensity takes place when a sample was subjected to x-ray exposure. From these angles we could find out changed spacing between diffraction planes due to any kind of deformation, which corresponds to the magnitude of residual stress [29]. The measurement conditions for residual stress were as given below:

Pitch: 50 μm.

X-ray incidence angle: 25.0 deg

X-ray irradiation time (Setup): 90 s.

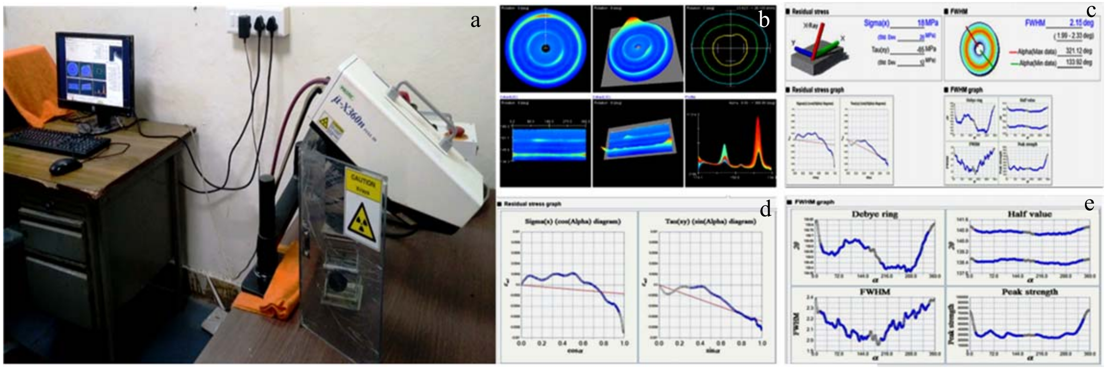

Figure 13. (a)–(e): Residual stress measurement using X-ray diffraction.

Table 8. Observations for residual stress and S/N ratio.

Residual stress (Mpa)					
Average residual stress in as-cast Al7075-T6 Specimen S0: 89					
Composite specimen	Reading 1	Reading 2	Reading 3	Mean	S/N ratio (dB)
S1	97	99	89	95	−39.56
S2	105	84	109	99.33	−39.99
S3	115	105	118	112.67	−41.05
S4	58	51	32	47	−33.67
S5	18	84	18	40	−34.10
S6	42	36	58	45.33	−33.31
S7	42	14	54	36.67	−32.11
S8	36	13	14	21	−27.431
S9	65	55	85	68.33	−36.831

X-ray wavelength (K-Alpha): 2.29093 A.
X-ray irradiation time (Meas.): 47 s.
X-ray irradiation time (Max): 82 s.
Sample distance (Monitor): 29.000 mm
Total measurement count: 7498
Sample distance (Analysis): 29.611/30.304 mm
Detection sensitivity: 52.8%
Temperature: 35.88 deg Centigrade
Peak analysis method: Fitting Lorentz

In this experimental work, as-cast Al 7075-T6 specimen and hybrid composite specimens (all in three replications) were characterized for residual stresses. Table 8 shows signal to noise ratio calculation from experimental data (three set of observations for three replications) for residual stress as 'smaller the better' type of quality characteristic of developed composites. In current investigation, all the residual stresses were found to be compressive in nature and it was noticed that generally residual stresses are lower for composites with higher reinforcement content.

Effects of all the process parameters considered during composite fabrication on S/N ratio and residual stress were studied and plotted as in figure 14. Graph in figure 14(a) displays that on increasing wt% of eggshell, residual stress in composites was decreased whereas from figures 14(b)–(d) it can be observed that on increasing SiC wt%, Al_2O_3 wt% and mechanical stirring time residual stress in composites was increased. Various graphs from figure 14 explain that for minimum residual stress in synthesized hybrid aluminium composites and S/N ratio optimum process parameter levels were 3rd level of eggshell content (A_3), 1st level of SiC content (B_1), 1st level of Al_2O_3 content (C_1) and 2nd level of mechanical stirring time (D_2). ANOVA at 95% confidence level was carried out to study effect of process parameters on utility function. Table 9 shows percentage contribution and F-ratio of different factors affecting the residual stress. It was realized from table 9 that eggshell wt% with percentage contribution P = 64.66% and SiC wt% with percentage contribution P = 28.42% influence the residual stressses significatly whereas Al_2O_3 wt% with percentage contribution P = 6.30% had moderate effect on residual stresses induced in synthesized hybrid composites. On the other hand, mechaincal stirring time had

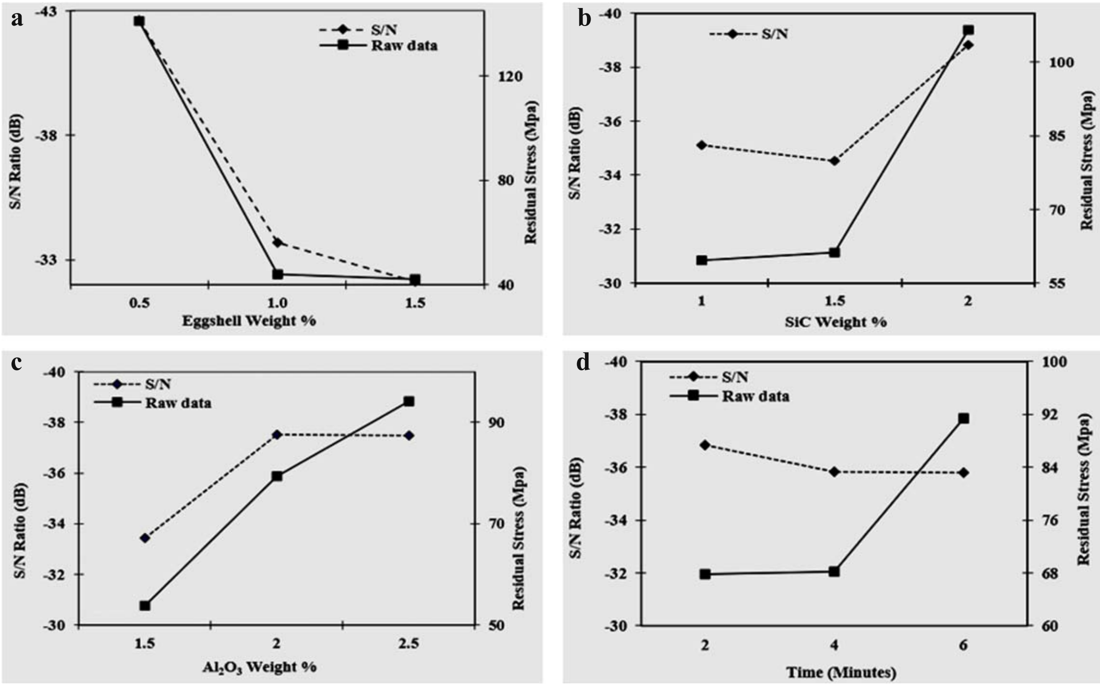

Figure 14. Effect of (a) Eggshell wt% (b) SiC wt% (c) Al_2O_3 wt% (d) mechanical stirring time on residual stress and S/N ratio.

Table 9. Analysis of variance (ANOVA) for residual stress.

Factor	Sum of squares (SS)	Degrees of freedom	Variance (V)	Percentage contribution (P)	F-Ratio
Eggshell Wt%	57840.22	2	28920.11	64.66	2266.52
SiC Wt%	25422.35	2	12711.18	28.42	996.2
Al_2O_3 Wt%	5635.65	2	2817.83	6.30	220.84
Stirring time	326.77	2	163.36	0.37	12.80
Others/errors	229.67	18	12.76	0.26	—
Total	89454.67	26	—	100	—

negligible influence on residual stresses. The main effect plots shown in figure 14 display that predominent control factors (eggshell wt%, SiC wt% and Al_2O_3 wt%) had highly inclined lines as compared to the insignifcant control factor. S/N ratio and mean response characteristics analysis was conducted followed by realization of optimum levels of significant factors as A_3, B_1 and C_1 for prediction of mean residual stress (X_{mp}). Following response average components were evaluated using experimental data from table 8.

$$\overline{G} = 62.81,\ \overline{A_3} = 42.0,\ \overline{B_1} = 59.56 \text{ and } \overline{C_1} = 53.78$$

$$X_{mp} = \overline{G} + (\overline{A_3} - \overline{G}) + (\overline{B_1} - \overline{G}) + (\overline{C_1} - \overline{G}) \tag{6}$$

Predicted mean optimum value of residual stress $X_{mp} = 29.70$ Mpa was calculated form equation (6). From table 9, error variance = 12.76 and DOF for error = 18 were obtained. F-ratio value at 95% confidence interval was determined from standard statistical table. The confidence interval (CI) calculated was ±6.13. Confidence interval with respect to 95% confidence level of predicted optimum residual stress was 23.57< Residual Stress (RS in Mpa) <35.83. Additionally a confirmation experiment was carried out by running three more replications for residual stress in developed hybrid composites at optimal levels of process parameters. Results of confirmation experiment were reported in table 10 and it was realized that mean value of residual stress 31.5 Mpa fell within the confidence interval 23.57< RS (Mpa) <35.83.

3.3. Prediction of optimum Microhardness in fabricated hybrid composites

Each of the specimens (one as-cast Al 7075-T6 specimen and nine hybrid specimens, in three replications) was tested for microhardness (on Fischer HM 2000S). During microhardness test a load of 300 mN was applied for 20 seconds keeping creep time 5 seconds and load release time 20 seconds. The microhardness of as-cast Al 7075-T6 specimen and composite specimens (in three replications) with varying reinforcement ratios along

Table 10. Confirmation experiment for residual stress.

Quality characteristic Residual stress in composites	Replications			Mean
	Replication 1	Replication 2	Replication 3	
	37.1	29.9	27.5	31.5

Table 11. Observations for microhardness and S/N ratio.

Microhardness (VHN)					
Average microhardness of as-cast Al7075-T6 Specimen S0: 167.5					
Composite specimen	Reading 1	Reading 2	Reading 3	Mean	S/N ratio (dB)
S1	196.5	197.7	196.5	196.9	44.12
S2	205.55	212.55	207.55	208.55	44.62
S3	215.5	218.6	217.8	217.3	44.97
S4	212.29	210.29	211.39	211.32	44.73
S5	229.01	229.01	230.01	229.34	45.44
S6	277.52	278.52	280.52	278.85	47.14
S7	226.34	228.34	238.34	231.00	45.50
S8	303.25	309.25	307.25	306.58	47.96
S9	286.4	286.4	288.4	287.06	47.39

Table 12. Analysis of variance (ANOVA) for microhardness.

Factor	Sum of squares (SS)	Degrees of freedom	Variance (V)	Percentage contribution (P)	F-Ratio
Eggshell Wt%	20394.81	2	10197.40	54.38	1279.29
SiC Wt%	11103.67	2	5551.83	29.44	696.49
Al_2O_3 Wt%	5833.95	2	2916.97	15.49	365.94
Stirring time	262.53	2	131.26	0.69	16.46
Others/errors	143.48	18	7.97	0.38	—
Total	37738.46	26	—	100	—

with S/N ratio calculation for 'larger the better' type of quality characteristic are given in table 11. Simultaneously, effects of various process parameters on S/N ratio and mean response were investigated and plotted as in figure 15. Figures 15(a)–(d) display that on increasing wt% of eggshell, wt% of SiC particles and mechanical stirring time, hardness of composites was increased. Whereas plot in figure 15(c) exhibits that composites hardness was decreased with increasing wt% of Al_2O_3 particles. It was observed from figure 15 that for maximum microhardness and S/N ratio, 3rd level of eggshell content (A_3), 3rd level of SiC content (B_3), 1st level of Al_2O_3 content (C_1) and 3rd level of mechanical stirring time (D_3) were optimum levels.

Table 12 represents ANOVA results for microhardness measurements performed at 95% confidence level in terms of F-ratio and percentage contribution of various factors. Microhardness of synthesized hybrid composites appeared to be influenced significantly by two control factors i.e. eggshell wt% ($P = 54.38\%$) and SiC wt% ($P = 29.44\%$) while the third control factor Al_2O_3 wt% ($P = 15.49\%$) had moderate effect on it. The fourth control factor mechanical stirring time could maginally affect the microhardness of composites. The graphs in figure 15 demonstrate that momentous control factor lines (eggshell wt%, SiC wt% and Al_2O_3 wt%) had elevated slopes whereas the insignifcant control factor mechanical stirring time had almost horizontal line. To compute predicted mean of microhardness (X_{mp}), S/N ratio and mean response characteristics analysis was conducted followed by realization of optimum levels of significant factors as A_3, B_3 and C_1. In current study for microhardness of developed hybrid composites following response average components were evaluated using experimental data from table 11.

$$\overline{G} = 240.77, \ \overline{A_3} = 274.89, \ \overline{B_3} = 261.07, \ \overline{C_1} = 260.78$$

$$X_{mp} = \overline{G} + (\overline{A_3} - \overline{G}) + (\overline{B_3} - \overline{G}) + (\overline{C_1} - \overline{G}) \quad (7)$$

From equation (7) predicted mean optimum value of microhardness X_{mp} was observed to be 315.20. Table 12 demonstrates values of error variance (7.97) and DOF for error (18). F-ratio value at 95% confidence

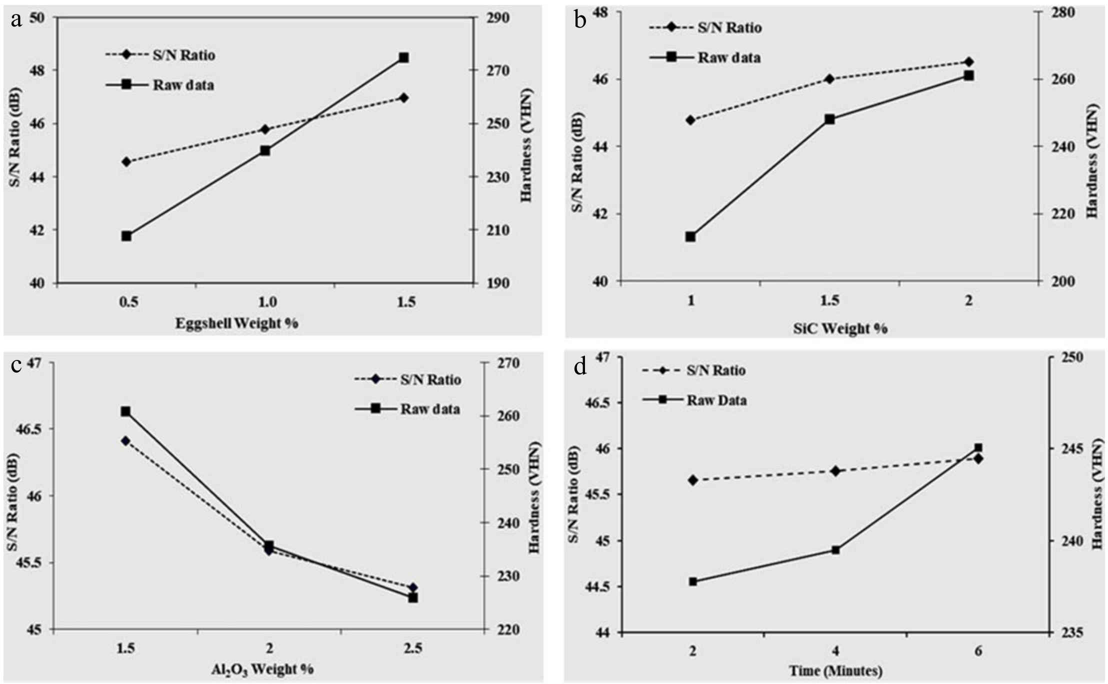

Figure 15. Effect of (a) Eggshell wt% (b) SiC wt% (c) Al_2O_3 wt% (d) mechanical stirring time on microhardness and S/N ratio.

Table 13. Confirmation experiment for microhardness.

Quality characteristic Microhardness of composites	Replications			Mean
	Replication 1	Replication 2	Replication 3	
	309.43	297.55	329.85	312.28

interval was determined from standard statistical table. The computed confidence interval (CI) was ±4.84. Therefore the confidence interval with respect to 95% confidence level of predicted optimum microhardness was 310.36 < H (Vickers Hardness Number) < 320.04. The confirmation experiment was done by running three more replications for microhardness of developed hybrid composites at optimal levels of process parameters and it was noticed that mean value of microhardness 312.28 as reported in table 13 was lying within the confidence interval 310.36 < H (VHN) < 320.04.

3.4. Prediction of optimum tensile strength of fabricated hybrid composites

In order to investigate the tensile behaviour of developed hybrid aluminium composites, specimens (in three replications) were characterized as per ASTM E8-M11 for ultimate tensile strength on universal testing machine (Tinius Olsen, H 50 K-S, Cross head speed: 2.5 mm min^{-1}, Strain rate : 0.002 s^{-1}). Each specimen was subjected to axial tensile load and the ultimate tensile strength value was observed, one of the fractured specimens is shown in figure 16. The ultimate force ranged from 876 N to 1520 N and the ultimate tensile strength was observed to be improving with infusion of reinforcement particles. Stress-strain diagrams of as-cast Al 7075-T6 alloy and composites are shown in figure 17. To analyse mean response function, signal to noise ratios ('larger the better' type of quality attribute) calculated from designed experimental data are expressed in table 14. Analysis of variance was performed to observe the impact of control factors on quality attribute. The effects of process parameters on tensile strength and S/N ratio have been plotted in figure 18. Figures 18(a)–(d) display that on increasing wt% of eggshell, wt% of SiC particles and mechanical stirring time, tensile strength of composites was increased. Whereas plot in figure 18(c) exhibits that composites tensile strength was decreased with increasing wt% of Al_2O_3 particles.

It was experienced that all the process parameters have a significant effect on utility function and the optimum levels are 3rd level of eggshell content (A_3), 2nd level of SiC content (B_2), 1st level of Al_2O_3 content (C_1) and 3rd level of mechanical stirring time (D_3). Table 15 demonstrates ANOVA results at 95% confidence level in

Figure 16. Fractured tensile test specimen.

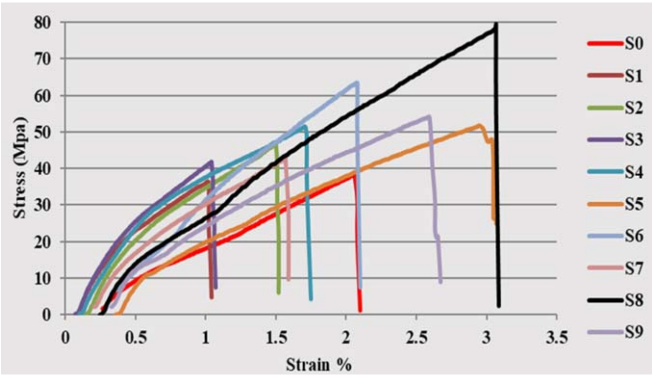

Figure 17. Stress-Strain diagram.

Table 14. Observations for tensile strength and S/N ratio.

Tensile strength (Mpa)					
Average tensile strength of as-cast Al7075-T6 Specimen S0: 38.3					
Composite specimen	Reading 1	Reading 2	Reading 3	Mean	S/N ratio (dB)
S1	36.7	34.6	38.3	36.5	30.73
S2	47.5	45.6	47.2	46.7	31.67
S3	40.9	42.9	41.9	41.9	31.08
S4	55.4	46.2	51.9	51.3	28.25
S5	44.3	56.1	54.9	51.8	31.55
S6	70.3	63.8	55.7	63.3	32.59
S7	43.1	50.1	34.7	42.6	30.70
S8	84.1	82.1	72.4	79.5	37.54
S9	49.7	54.6	58.1	54.1	33.70

terms of F-ratio and percentage contribution of process parameters. By analyzing S/N ratio and mean response characteristic, significant control value optimum levels were identified as A_3, B_2 and C_1.

Control factors eggshell content with percentage contribution $P = 27.22\%$, Silicon Carbide content with percentage contribution $P = 25.81\%$ and Aluminium Oxide content with percentage contribution $P = 21.36\%$ had impactful influence on tensile strength of hybrid composites while mechaincal stirring time had imperceptible effect on it. The plots shown in figure 18 demonstrate that dominating control factors (eggshell wt%, SiC wt% and Al_2O_3 wt%) had lines with higher inclinations in comparison of the insignifcant control factor. For estimation of predicted mean of tensile strength (X_{mp}), equation (8) is used after putting the values of following response average components from table 14:

$$\overline{G} = 51.97,\ \ \overline{A_3} = 58.8,\ \ \overline{B_2} = 59.4\ ,\ \ \overline{C_1} = 59.8$$

$$X_{mp} = \overline{G} + (\overline{A_3} - \overline{G}) + (\overline{B_2} - \overline{G}) + (\overline{C_1} - \overline{G}) \tag{8}$$

From equation (6), predicted mean optimum value of tensile strength X_{mp} was computed to be 74.0 Mpa. Table 15 shows error variance = 79.80 and DOF for error = 18. For F-ratio evaluation at 95% confidence interval standard statistical table was used. The calculated confidence interval (CI) obtained was ±15.32. Hence the confidence interval with respect to 95% confidence level of predicted optimum tensile strength was 58.68<

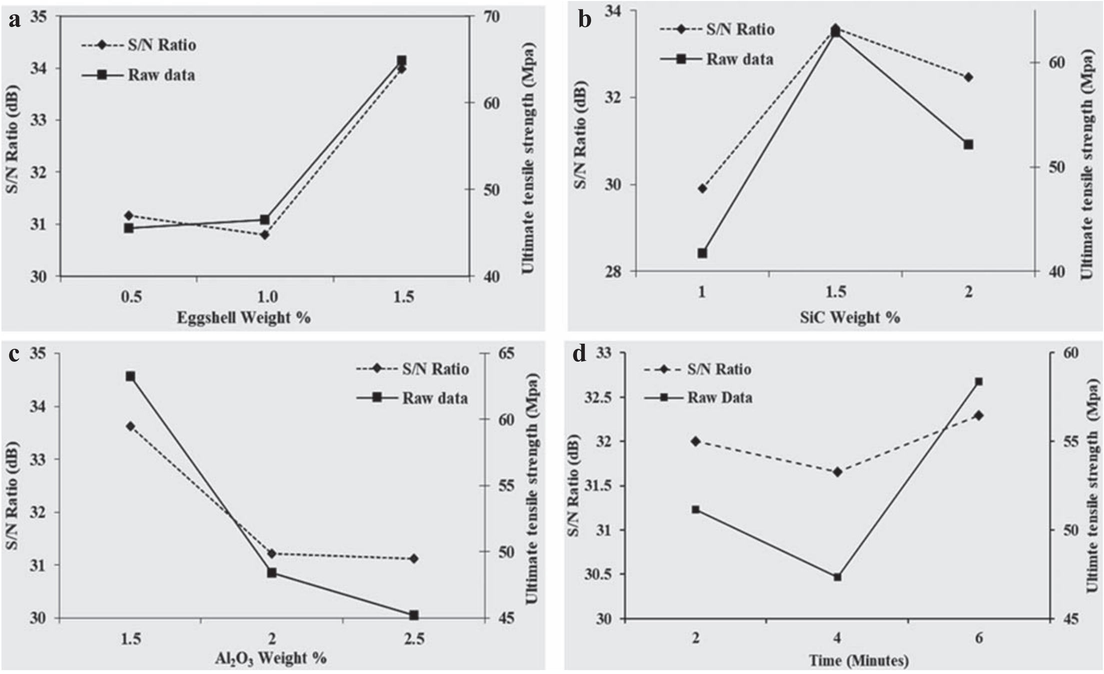

Figure 18. Effect of (a) Eggshell wt% (b) SiC wt% (c) Al_2O_3 wt% (d) mechanical stirring time on tensile strength and S/N ratio.

Table 15. Analysis of variance (ANOVA) for tensile strength.

Factor	Sum of squares (SS)	Degrees of freedom	Variance (V)	Percentage contribution (P)	F-Ratio
Eggshell Wt%	2133.43	2	1066.71	27.22	13.37
SiC Wt%	2022.66	2	1011.33	25.81	12.67
Al_2O_3 Wt%	1674.40	2	837.20	21.36	10.49
Stirring time	570.90	2	285.45	7.28	3.58
Others/errors	1436.48	18	79.80	18.33	—
Total	7837.89	26	—	100	—

Table 16. Confirmation experiment for tensile strength.

Quality characteristic	Replications			
Tensile strength of composites	Replication 1	Replication 2	Replication 3	Mean
	68.26	75.32	60.25	67.94

Tensile Strength (TS in Mpa) < 89.32. It was followed by a confirmation experiment by running three more replications for tensile strength of developed hybrid composites at optimal levels of process parameters and it was observed that mean value of tensile strength 67.94 Mpa as reported in table 16 was lying within the confidence interval 58.68< TS (Mpa) < 89.32.

3.5. Metallographic analysis

Among fabricated composites, composite specimen S8 (Al 7075-T6/1.5 wt% eggshell/1.5 wt% SiC/1.5 wt% Al_2O_3/Mechanical stirring time 6 min) exhibited outstandingly enhanced mechanical properties in terms of lowest percentage porosity, lowest residual stress, highest micro-hardness and highest tensile strength. For comparative studies, XRD plots, EDS profiles and Raman spectra of as-cast Al 7075-T6 specimen S0 and hybrid composite specimen S8 demonstrating their elemental composition without any oxygen and carbon content are shown in figures 19–21. FESEM images of as-cast Al 7075-T6 specimen S0 and hybrid composite specimen S8 are shown in figure 22. The micrograph of base alloy displayed uniform fine grain sizes whereas in composite along with reinforcement traces, occurrence of some uneven grains may be associated with infusion of reinforcement particles. From figure 22, composite microstructure appeared to have homogenous distribution

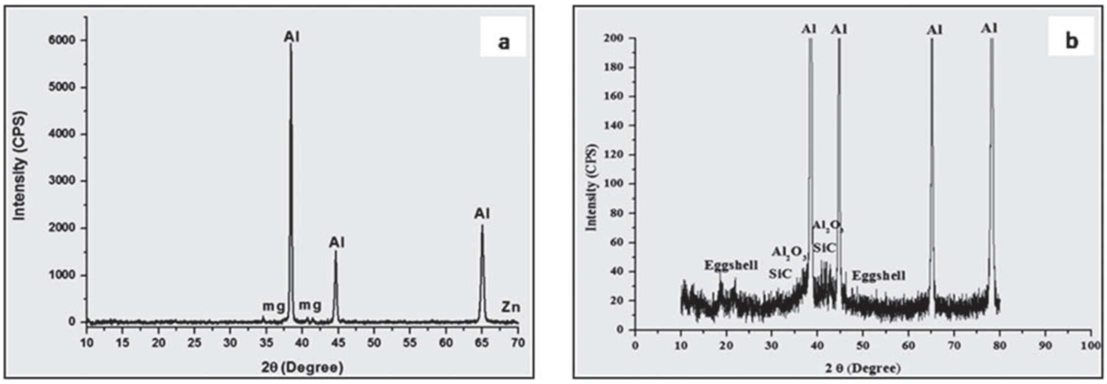

Figure 19. XRD patterns of (a) As-cast Al 7075-T6 specimen S0 (b) Composite specimen S8.

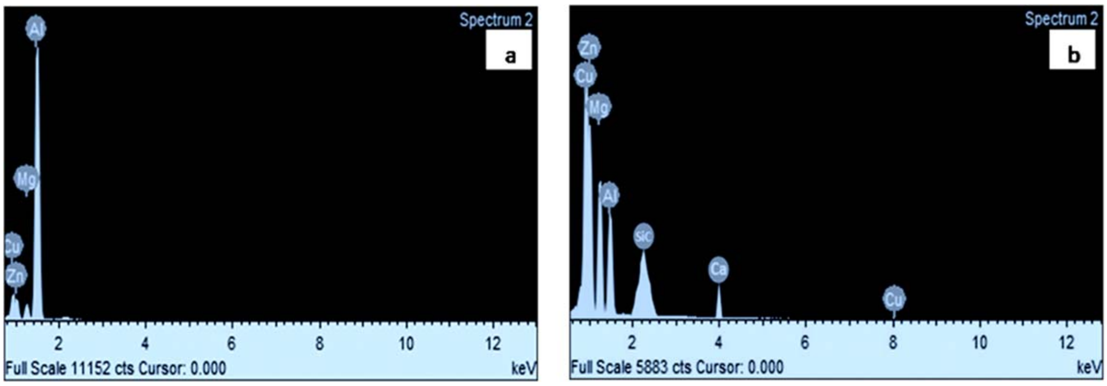

Figure 20. EDS profiles of (a) As-cast Al 7075-T6 specimen S0 (b) Composite specimen S8.

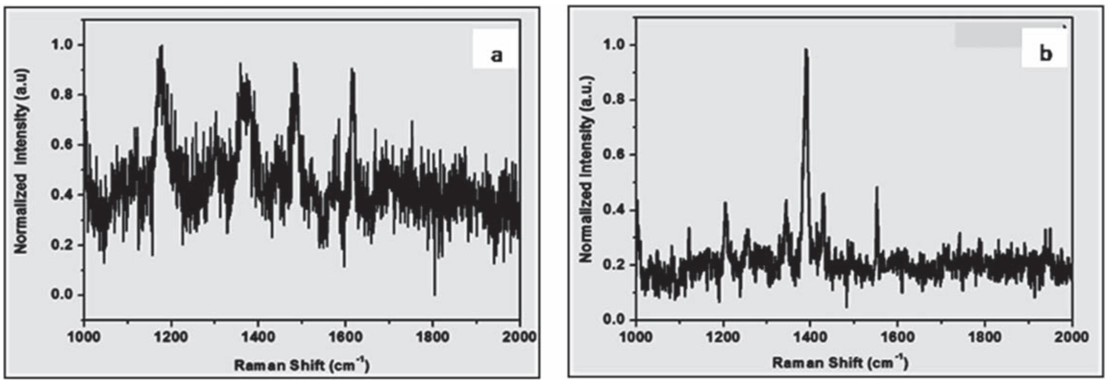

Figure 21. Raman spectra of (a) As-cast Al 7075-T6 specimen S0 (b) Composite specimen S8.

of filler particles, but the occurrence of particle clusters could not be ignored due to agglomeration. Synthesized composites also exhibited some traces of porosity due to various process induced effects such as gas trapped in metal melt during mixing, shrinkage due to composites solidification, presence of moisture on reinforcement particles surfaces, evolution of hydrogen and inappropriate casting parameters during fabrication creating isolated areas in composites which get solidify at last and generate voids. Porosity reduces the mechanical attributes of composites due to occurrence of stress concentration in proximity of voids [30]. To reduce porosity, a balance is necessary between void sources (trapped air and moistures layers etc) and voids sink (vacuum evacuation and bubble mobility etc). Comparative reduction in porosity with reinforcement addition to metal matrix is shown in figure 23. In general, residual stresses or strain fields are developed within the

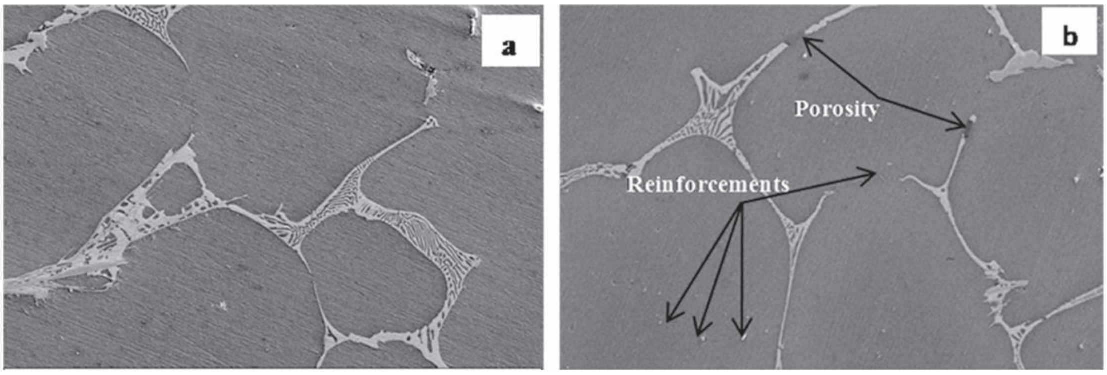

Figure 22. FESEM images of (a) As-cast Al7075-T6 specimen S0 (b) composite specimen S8.

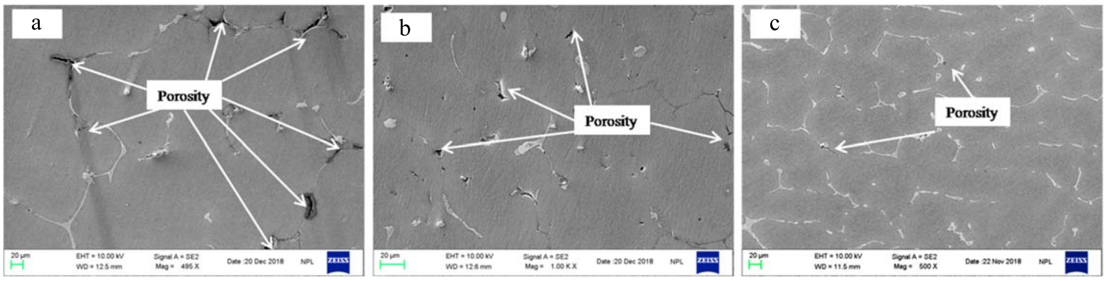

Figure 23. Porosity in microstructure (a) As-cast Al 7075-T6 specimen S0 (b) Hybrid composite specimen S5 (c) Hybrid composite specimen S8.

composites because of thermomechanical mismatch in the characteristics of metal matrix and reinforcement during cooling from fabrication temperature, presence of moisture, fluctuation in material properties, difference in amount of reinforcement and tool-part interaction during machining [31]. Variations in residual stresses of fabricated hybrid composites may primarily be associated with thermal residual stresses during electromagnetic stir casting process, distinct weight percentage of reinforcements infused and residual stresses developed during machining of hybrid composites. Lower values of residual stress in hybrid composites may be because of increased dislocation density due to higher reinforcement content [32]. Specimens S0 was subjected to higher residual stresses while specimens S8 with higher filler content exhibited lower residual stresses. Specimen S3 was an exception with higher reinforcement content and higher residual stress and this possibility may be attributed to the phenomenon of plastic deformation which got enhanced with reduced dislocation density. As compared to the unreinforced metal matrix, the presence of reinforcement particles in base metal restrains mechanical dislocations within the composites [33, 34] causing enhanced strength and hardness. All the composite specimens showed improved microhardness as compared to the unreinforced base metal specimen S0, due to the hardness properties of incorporated reinforcement particles (predominantly eggshell and SiC particles). It was ascertained from current experimental data that as percentage porosity increased, hardness and tensile strength of fabricated hybrid composites decreased due to failure inception from voids within composites. Here as- cast Al7075-T6 specimen S0 with maximum percentage porosity showed lower microhardness and tensile strength while hybrid composite specimen S8 with higher reinforcement contents, longer stirring time and lesser percentage porosity demonstrated higher microhardness and tensile strength. In exceptional case, ultimate tensile strength of a composite specimen S1 was observed to be lesser than that of base metal (specimen S0) and it may be as a result of formation of loosely bound reinforcement particle micro-clusters due to agglomeration and porosity. In case of hybrid composites specimen S7, reduced ductility may be due to infusion of hard SiC and Al_2O_3 particles concentrating stress at metal matrix-reinforcement interface and localizing crack initiation resulting into brittleness. In some of the SEM micrographs of fractured specimens shown in figure 24, detached reinforcement particles were found due to the breakage of bonds between metal matrix and reinforcements. The fractured surfaces were observed to exhibit cup-cone mode of fracture, which substantiated that the fracture occurred was somewhat ductile in nature and necking of tensile test specimen under axial load eventuated before the metal matrix failure took place [35, 36].

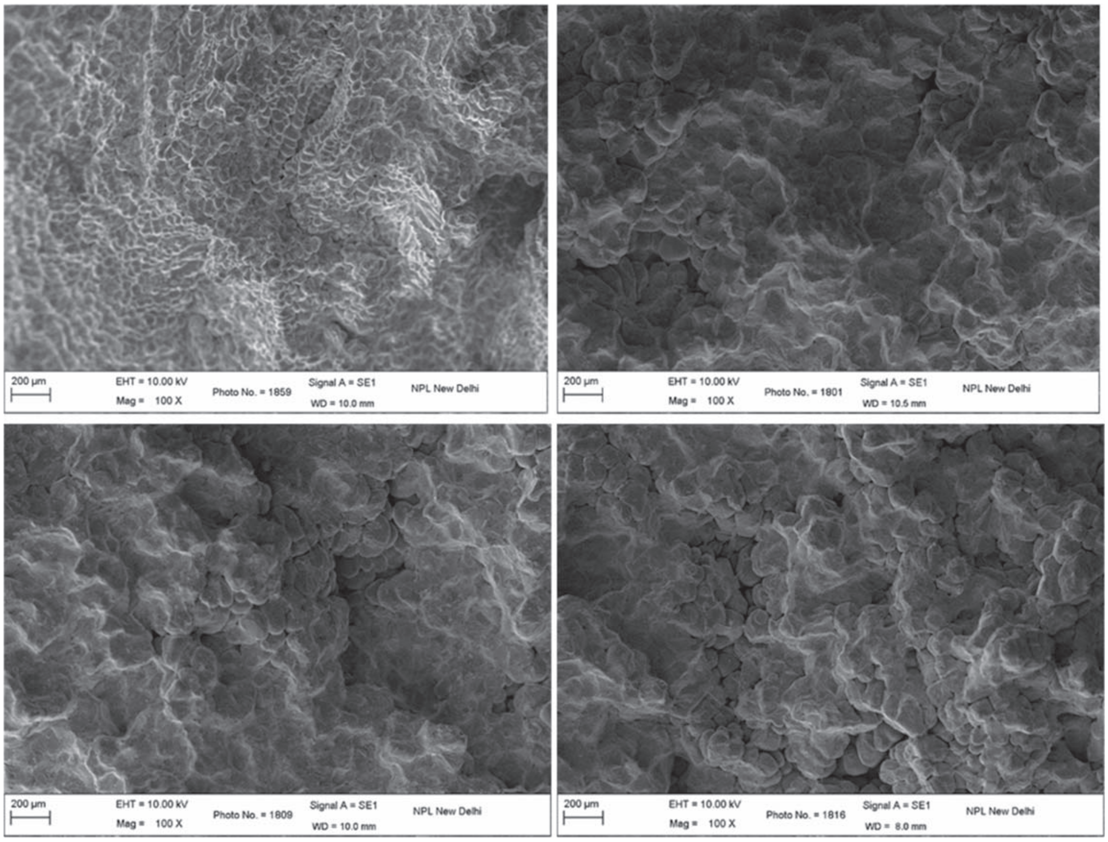

Figure 24. SEM micrographs of fracture surfaces of composite specimen after tensile test.

4. Conclusion

Al 7075-T6/Eggshell/SiC/Al_2O_3 hybrid composites with variable reinforcement's content and mechanical stirring time were developed successfully as per the design matrix by electromagnetic stir casting technique. Use of hazardous eggshell waste as reinforcement resulted into synthesis of ecodesigned and economical hybrid composites with augmented physical and mechanical attributes. Each composite specimen exhibited distinctive enhanced property, hence to be considered as viable alternate material for potential engineering applications.

- No significant change in density of composites was observed as compared to the base metal (only upto 2.2%).
- The maximum decrease in percentage porosity of synthesized hybrid composites was upto 75% as compared to as-cast Al 7075-T6 with optimum levels of significant factors (Eggshell wt%:1.5 and mechanical stirring time: 4 min). Predicted optimum value of percentage porosity for 95% confidence interval was $0.121 < PP < 0.5$ with mean value of percentage porosity $= 0.39$ from confirmation experiment corresponding to optimum conditions, which fell within the predicted confidence interval as per Taguchi's parameter design technique predictions.
- A maximum decrease in residual stress in composites was observed to be 76% as compared to as-cast Al 7075-T6 specimen. Eggshell wt%: 1.5, SiC wt%: 1 and Al_2O_3 wt% 1.5 were the optimum levels of significant process parameters. Predicted optimum value of residual stress for 95% confidence interval was $23.57 < RS$ (Mpa) < 35.83 with mean value of residual stress $= 31.5$ Mpa obtained from confirmation experiment corresponding to optimum conditions according to Taguchi's parameter design technique predictions.
- An enhancement of maximum 83% in microhardness of prepared hybrid composites was witnessed as compared to its unreinforced counterpart. The optimum levels of dominant process parameters were observed to be as eggshell wt%: 1.5, SiC wt%: 2 and Al_2O_3 wt%: 1.5. Predicted optimum value of microhardness for 95% confidence interval was $310.36 < H$ (VHN) < 320.04 with mean value of microhardness $= 312.28$ from confirmation experiment corresponding to optimum conditions of process parameters, establishing a good agreement between Taguchi's parameter design technique predictions and confirmation experiment outcomes.

- There is an increase of maximum 107% in tensile strength of fabricated hybrid composites specimen as compared to the as-cast Al 7075-T6 specimen. The significant process parameters have optimum levels as eggshell wt%: 1.5, SiC wt%: 1.5 and Al_2O_3 wt%: 1.5. Predicted optimum value of tensile strength for 95% confidence interval was $58.68 < TS\ (Mpa) < 89.32$ with mean value of tensile strength $= 67.94$ Mpa from confirmation experiment corresponding to optimum conditions of process parameters as per Taguchi's parameter design technique predictions.

Acknowledgments

Authors are thankful to DNPL for his constant support and encouragement. Authors would also like express their sincere thanks to IUAC, Delhi for providing characterization facilities.

ORCID iDs

Girija Moona https://orcid.org/0000-0001-9804-499X

References

[1] Yan C, Lifeng W and Jianyue R 2008 *CJA* **21** 578 (https://www.sciencedirect.com/science/article/pii/S1000936108601776)
[2] Christy T V, Murugan N and Kumar S 2010 *JMMCE* **9** 57
[3] Moona G, Walia R S, Rastogi V and Sharma R 2018 *IJPAP* **56** 164 (http://op.niscair.res.in/index.php/IJPAP/article/viewFile/17513/1465)
[4] Singla M, Dwivedi D D, Singh L and Chawla V 2009 *JMMCE* **8** 455
[5] Bhushan R K, Kumar S and Das S 2013 *Int J Adv Manuf. Technol.* **65** 611
[6] Poovazhagan L, Kalaichelvan K and Rajadurai A 2013 *Procedia. Eng.* **64** 681
[7] Pitchayyapillai G, Seenikannan P, Balasundar P and Narayanasamy P 2017 *Trans Nonferrous Met Soc China* **27** 2137
[8] Adeosun S O, Osoba L O and Taiwo O O 2014 *Int J Chem, Mol., Nucl. Mat. Metall. Eng.* **8** 731 (https://publications.waset.org/10000007/characteristics-of-aluminum-hybrid-composites)
[9] Balasivanandha S P, Karunamoorthy L, Kathiresan S and Mohan B 2006 *J. Mater. Process Technol.* **171** 268
[10] Li M J, Tamura T, Omura N and Miwa K 2010 *Trans. Nonferrous Met. Soc. China* **20** 1192
[11] Ravindran R, Manisekar K, Narayanasamy P, Selvakumar N and Narayanasamy R 2012 *Mater Des.* **39** 42
[12] Clark R Jr, Coughran B, Traina I, Hernandez A, Scheck T, Etuk C, Peters J, Lee E W, Ogren J and Es-Said O S 2009 *Eng. Fail. Anal.* **12** 520
[13] Gan Y X 2009 *Int. J. Mol. Sci.* **10** 5115
[14] Veeresh Kumar G B, Rao C S P, Selvaraj N and Bhagyashekar M S 2010 *JMMCE* **9** 43
[15] Buntan R, Phuenchomphu D, Sukmoung P, Doomao K, Anunapiwat O and Patcharawit T 2011 *JMMM* **21** 73 (http://ojs.materialsconnex.com/index.php/jmmm/article/view/188/215)
[16] Lashgari H R, Emamy M, Razaghian A and Najimi A A 2009 *Mater. Sci. Eng.* A **517** 170
[17] Parlevliet P, Bersee H and Beukers A 2006 *Composites Part* A **37** 1847
[18] Kok M 2005 *J. Mater. Process Techno.* **161** 381
[19] http://asm.matweb.com/search/SpecificMaterial.asp?bassnum=ma7075t6 (accessed in January 2019)
[20] Walia R S, Shan H S and Kumar P 2006 *Mater. Manuf. processes* **21** 375
[21] Walia R S, Shan h S and Kumar P 2006 *Mach. Sci. Technol.* **10** 341
[22] Ahmad S N, Hashim J and Ghazali M I 2005 *J. Compos. Mater.* **39** 451
[23] Selvakumar N and Narayanasamy P 2016 *Tribol. T.* **59** 733
[24] Brar B S, Walia R S and Singh V P 2015 *Int. J. Adv. Manuf. Tech.* **79** 329
[25] Narayanasamy P and Selvakumar N 2017 *J. Tribol.-ASME* **139** 051301
[26] Ravindran P, Manisekar K, Narayanasamy R and Narayanasamy P 2013 *Ceram. Int.* **39** 1169–82
[27] Singh H and Kumar P 2004 *Indian. J. Eng. Mater. Sci.* **11** 19 (http://nopr.niscair.res.in/bitstream/123456789/9256/1/IJEMS%2011%281%29%2019-24.pdf)
[28] Goyal T, Walia R S and Sidhu T S 2013 *Int J Adv Manuf Tech* **64** 903
[29] Withers P J and Bhadeshia H K D H 2000 *Mater. Sci. Tech* **17** 355
[30] Centea T and Hubert P 2012 *Composites Part* A **43** 1505
[31] Guzmán R E and Hernández Arroyo E 2016 *J. Phys.: Conference Series* **687** 012060
[32] Liu H T and Sun L Z 2004 *Int. J. Solid. Struct.* **41** 2189
[33] Suresh K R, Niranjan H B, Martin Jabraj P and Chowdaiah M P 2003 *Wear* **255** 638
[34] Wong W L E, Gupta M and Lim C Y H 2006 *Mater. Sci. Eng.* A **423** 148
[35] Huang H, Tsutsumi S, Wang J, Li L and Murakawa H 2017 *Finite. Elem. Anal. Des.* **135**
[36] Su H, Gao W, Feng Z and Lu Z 2012 *Mater. Des.* **36** 590